

DETERMINATION OF THE QUANTITY OF EARTH'S
GRAVITY IMPARTED ON PARTICLES IN A
ROTATING CYLINDER FLUID REGIME BASED ON
PARTICLE DENSITY AND ROTATION SPEED

By

DEVIN M. JURKO

Bachelor of Science in Mechanical Engineering

Oklahoma State University

Stillwater, Oklahoma

2020

Submitted to the Faculty of the
Graduate College of the
Oklahoma State University
in partial fulfillment of
the requirements for
the Degree of
MASTER OF SCIENCE
May, 2023

DETERMINATION OF THE QUANTITY OF EARTH'S
GRAVITY IMPARTED ON PARTICLES IN A
ROTATING CYLINDER FLUID REGIME BASED ON
PARTICLE DENSITY AND ROTATION SPEED

Thesis Approved:

Dr. Aaron Alexander

Thesis Adviser

Dr. Hitesh Vora

Dr. Chulho Yang

ACKNOWLEDGEMENTS

I would like to express my deepest appreciation and gratitude to my co-authors, Jeremy Sabo, Dr. Alexander, and Dr. Miller, for their invaluable support and guidance throughout the duration of this project. Their knowledge and expertise have been instrumental in shaping this thesis and making it possible. I am truly grateful for their encouragement and wisdom, which has helped me to grow both professionally and personally.

I would also like to extend a special thanks to Dr. Vora and Dr. Yang for their contributions as members of my Thesis Committee. Their insightful comments and feedback have been critical in improving the quality of this work.

I would also like to thank my family and friends for all of their support though this process. I truly could not have done it without them, and I am extremely grateful to have had them by my side throughout this process.

I am grateful to Dr. Agnew for his generous help and feedback on the different versions of my thesis. His expertise and attention to detail have helped me to refine my arguments and strengthen the overall presentation of my research.

Furthermore, I would like to express my sincere gratitude to NASA for providing funding to OSU through grant number 80NSSC19K0428. This grant funded the work in which this work was an extension of.

Finally, I would like to acknowledge the High-Performance Computing Center at Oklahoma State University, which supported this project in part through the National Science Foundation grant OAC-1126330. Their resources were essential in the completion of this work, and I am grateful for their continued support of scientific research.

Thank you all for your contributions to this project. Without your help, this thesis would not have been possible.

Name: Devin M. Jurko

Date of Degree: May, 2023

Title of Study: DETERMINATION OF THE QUANTITY OF EARTH'S GRAVITY
IMPARTED ON PARTICLES IN A ROTATING CYLINDER FLUID REGIME
BASED ON PARTICLE DENSITY AND ROTATION SPEED

Major Field: Engineering Technology

Abstract: This research is an in-depth analysis of the movement of yeast-like particles in a Rotating Wall Vessel (RWV) using a series of computational fluid dynamic (CFD) simulations. The purpose of the RWV is to counteract the effects of gravity by reducing the internal and external effects that it has on particles in cultures, in this case spherically modeled simulated yeast cells. The internal effects can be characterized as the distortion of the internal structure due to density differences, whereas the external effect results from the deformations of the particle shape resulting from collisions with the RWV walls or other particles. The RWV counteracts both effects by continuously rotating the fluid regime containing the cellular particles, allowing for a constant state of particle suspension. Using CFD simulations, an RWV with yeast cells in the fluid regime was modeled to track the acceleration and movement of these particles at various locations within the unit. Our analyses found that depending on their location in the vessel, the particles experienced different accelerations. The particle acceleration was the smallest towards the center of the fluid regime where the particles were furthest away from the walls. Specifically, the particles experienced between 0 m/s^2 and $.2 \text{ m/s}^2$, meaning that the RWV can successfully counteract 98-100% of the acceleration due to the gravity of Earth. This work creates a repeatable framework for the analysis of how cells move in a RWV to help understand the gravitational forces that the cells experience that may trigger certain biological responses.

TABLE OF CONTENTS

Chapter	Page
I. INTRODUCTION.....	1
II. REVIEW OF LITERATURE.....	4
2.1 Types of Cell Culture Vessels.....	4
2.2 Multicellular Applications	6
2.3 Importance of Yeast in the RWV.....	8
2.4 Research Gap	8
III. METHODOLOGY	10
3.1 CFD Model	10
IV. RESULTS & DISCUSSION	20
V. CONCLUSION.....	33
5.1 Future Work	33
5.11 PIV (Particle Image Velocimetry)	33
5.12 A Framework to test different experimental set-ups.....	34
REFERENCES	35

LIST OF TABLES

Table	Page
Table 1: Static Sim -Particle Displacement v Calc Particle Displacement	29

LIST OF FIGURES

Figure	Page
Fig. 1: Nasa Designed Rotating Wall Vessel.....	3
Fig. 2: Geometry Scene of 0.1 in plane section	10
Fig. 3: Sim 1 – Particle Orientation at radial distance $r = 30$ mm	11
Fig. 4: Sim 2 – Particle Orientation at radial distance $r = 35$ mm	12
Fig. 5: Sim 3 – Particle Orientation at radial distance $r = 39$ mm	12
Fig. 6: Sim 4 – Particle Orientation at radial distance $r = 45$ mm	13
Fig. 7: Fully Developed fluid domain without particles	14
Fig. 8: Sim 1 – Mesh Scene for $r = 30$ mm.....	16
Fig. 9: Sim 2 – Mesh Scene for $r = 35$ mm.....	16
Fig. 10: Sim 3 – Mesh Scene for $r = 39$ mm.....	17
Fig. 11: Sim 4 – Mesh Scene for $r = 43$ mm.....	17
Fig. 12: Mesh Scene – Prism Layers	18
Fig. 13: Sim 1 – Particle Position Deviation $r = 30$ mm.....	20
Fig. 14: Sim 2 – Particle Position Deviation $r = 35$ mm.....	21
Fig. 15: Sim 3 – Particle Position Deviation $r = 39$ mm.....	21
Fig. 16: Sim 4 – Particle Position Deviation $r = 43$ mm.....	22
Fig. 17: Sim 1 – Calculated Particle Acceleration vs. Time $r = 30$ mm	23
Fig. 18: Sim 2 – Calculated Particle Acceleration vs. Time $r = 35$ mm	23
Fig. 19: Sim 3 – Calculated Particle Acceleration vs. Time $r = 39$ mm	24
Fig. 20: Sim 4 – Calculated Particle Acceleration vs. Time $r = 43$ mm	24
Fig. 21: Sim 1 – Calculated Particle Acceleration v Ang. Position $r = 30$ mm	26
Fig. 22: Sim 2 – Calculated Particle Acceleration v Ang. Position $r = 35$ mm	26
Fig. 23: Sim 3 – Calculated Particle Acceleration v Ang. Position $r = 39$ mm	27
Fig. 23: Sim 3 – Calculated Particle Acceleration v Ang. Position $r = 43$ mm	27
Fig. 25: Comparing Particle Velocity to Fluid Regime Velocity (Magnitude)	30
Figure 26: Standard Deviation of Calculated Acceleration vs Radial Position	31

CHAPTER I

INTRODUCTION

Rotating Wall Vessels (RWV) have gained much popularity in the scientific community for the many benefits they offer for growing cell aggregates. They allow for the cells to retain their specialized features by reducing the mechanical culture conditions induced on the particles, which also gives them a higher survival rate during the growing period (T. G. Hammond and J. M. Hammond, 2001). There are variety of these vessels that provide slightly different conditions

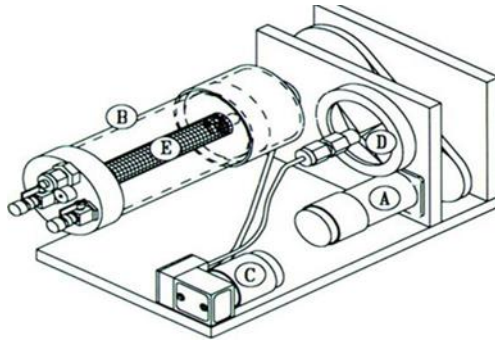


Figure 1: Nasa Designed Rotating Wall Vessel

for growing, each with their own benefits. The NASA designed rotating wall vessel (Fig. 1) provides solid body rotation that allows them to grow in a state of simulated microgravity, though particle suspension (Wolf DA, Schwartz RP, 1991). While grown in this state, the cells are suspended in a culture medium and do not deviate too far from each other, allowing them to form bridges without them getting ripped apart due to the fluid shear. (Schwarz RP, Goodwin TJ, Wolf DA, 1992). The cells can “feel” the difference in shear when induced to microgravity and they alter the structure of their spindle microtubules

(Wei, Diao, Qi, Khokhlov, Feng, Xing, & Li, 2013). The cells are able to grow evenly in all directions without the directional bias that is induced by the force of gravity. While it is important to understand that the cells react well in this type of environment because of the reduced fluid shear, it is just as important to understand exactly how these vessels achieve this on a deeper level. The way this vessel rotates about its central axis creates what is known as Coriolis and centrifugal forces, which act as the main driving factors of the system. Both forces are present when run in Earth's gravity but mostly eliminated in the actual microgravity of space (Wolf DA and Schwartz RP, 1991). This means that the force of gravity must be present for this system to work. After all, the whole point of this system is to counteract the acceleration that the particles experience due to gravity, so it would make sense that it would not work the same when there is no gravity to counteract. These two forces coupled with the buoyancy of the particles within the culture medium reduce the acceleration of the particles due to the Earth's gravity. These two forces account for a large portion of the flows and conditions that occur within this type of vessel.

A wide range of cellular systems are cultured in RWVs, this ranges from larger multicellular systems to smaller single cell systems. *Saccharomyces cerevisiae*, or budding yeast, is a single cell system that can be cultured in RWVs for the purpose of observing how microgravity affects its aging process. Since mammalian cells and yeast cells share many similarities on how they age, key findings that may improve the way yeast cells function in microgravity may be able to be directly applied to that of humans while conducting operations in space (Fukuda, Ana Paula, et al., 2021). Being able to quantify the exact downward acceleration of the yeast particles as they rotate in the RWV would provide a more comprehensive understanding exactly how much Earth's gravity the RWV can counteract. Yeast particles are typically too small to observe with the naked eye, as they typically range in size from around 8 to 14 μm when grown at a temperature of 30°C (Zakhartsev, Maksim, and Matthias Reuss., 2018).

The microscopic nature of these cells makes it nearly impossible to directly evaluate how the fluid flow regime affects them. There are different ways that have proven useful to calculate physics values in this type of fluid regime, some of which include computational fluid dynamics (CFD) and particle image velocimetry (PIV). CFD is an extremely useful tool for analyzing fluid regimes because it requires no real world set up and can be conducted completely virtually. PIV on the other hand, requires more experimental setup and the use of highly expensive materials, such as lasers and the materials needed to replicate the fluid regime being tested, but is still a very useful way of conducting fluid regime analyses. This paper will use computational fluid dynamics (CFD) to analyze the way yeast particles move through this type of fluid regime and determine what quantity of the acceleration due to Earth's gravity the RWV can successfully counteract. The ultimate goal of this study is 2-fold. The first being to provide supplemental information and a system validation to researchers who plan to conduct experiments that involve culturing yeast particles in RWVs for the sake of advancing the adaptability of humans in space. The second being to serve as a framework to allow future researchers to model different types of particles at different rotation speeds in a Rotating Wall Vessel.

CHAPTER II

REVIEW OF LITERATURE

2.1 Types of Cell Culture Vessels

There have been many different types of cell culture vessels that have been designed with the intention of allowing cells to grow in low shear environments. Some of which included an inlet and outlet which would allow for a constant stream of fresh culture medium to move through the system and others had the ability to have the inner and outer walls move independently of one another. These systems proved to be unideal due to certain types of flows that were discovered to increase the amount of fluid shear on the cell cultures. One of the main types of flows that was found to be present in these systems is Taylor-Couette flow, which is considered turbulent, and is optimized in vessels with counter rotating cylinders (Jalalabadi, Kim & Jin Sung, 2017). While not optimized, Taylor-Couette flow is also present in vessels with cylinders that are rotating the same direction with an inlet and outlet flow. Taylor Vortices are a byproduct of this type of turbulent flow and tend to be stronger towards the spin filter but have a higher population density towards the outer wall (Jalalabadi, Kim & Jin Sung, 2017). A CFD simulation was performed by (Figueredo-Cardero, A., Martínez, E., Chico, E., Castilho, L.R. and Medronho, R.A., 2014) which confirmed the existence of Taylor vortices and showed that the inlet flow comes in evenly distributed along the front of the vessel and the outlet flow is evenly distributed along the spin filter. Particle image velocimetry (PIV) was utilized to provide fluid dynamic data for a rotating cell culture system with inlet and exit flow. Using this imagery method, they were able to find

evidence of Taylor vortices and were able to confirm that there is turbulence in these types of systems (Figueredo-Cardero, A., Chico, E., Castilho, L. and de Andrade Medronho, R., 2012). The vessels that produce these types of flows do not provide the most ideal conditions for cell culture growth. The turbulence due to the strong Taylor Vortices causes a higher shear on the cells, typically leading to a higher percentage of damaged cells. This type of flow is only present in vessels with turbulent conditions, mainly caused by the presence of an inflow and outflow. While this is a very prominent type of flow that exists in many types of rotating vessels, there are vessels where these turbulent conditions are nearly eliminated by the removal of the inlet and outlet flow.

In vessels with solid body rotation, or SBR, the fluid medium is allowed to rotate along with the inner and outer wall at the same rate. For this to happen, the vessel cannot have an inlet or exit flow, must have the inner and outer cylinders rotating at the same speed, and must be completely filled with the culture medium and any gas present in the system must be eliminated (Schwarz RP, Goodwin TJ, Wolf DA., 1991). Running a vessel under these conditions eliminates the main mechanisms that cause turbulence in the system, meaning that rotating culture vessels with SBR can be considered to have laminar flow. This provides much better conditions for the cells to grow under due to the reduced shear stress, and increased mass transfer rates (M.N. Cinbiz, R.S. Tıǧlı, I.G. Beşkardeş, M. Gümüşderelioǧlu , Ü. Çolak, 2010). The conditions that vessels with SBR creates (reduced shear and turbulence) is comparable to the conditions presented in actual microgravity (Schwarz RP, Goodwin TJ, Wolf DA.). Growing cells in the actual microgravity of space is not always the most convenient option since most scientists do not have direct access to a rocket ship suited for space travel. This limits the type of experiments that can be conducted under the conditions provided by microgravity. Therefore, the NASA designed Rotating Wall Vessel with SBR has become the best when needing to grow cells in a microgravity environment.

2.2 Multicellular Applications

The NASA designed RWVs are used for many applications because of the benefits they offer regarding growing three dimensional cultures in a fully optimized low shear environment. They have opened an entirely new way to study the way different organisms react under certain growing conditions that are offered by the Rotating Wall Vessel. A study was conducted that tested the effectiveness of growing fetal liver samples from mice in one of these rotating wall vessels and compared the results to that of older methods of growing including the Hanging Drop and the Spinner Flask Method (Ishikawa, Momotaro, 2011). They cultured each of the samples for 10 days. The cell aggregates grown in the Hanging Drop Method did not have a smooth round shape and only had a few blood vessel-like structures that could be seen in the tissue. The Spinner Flask Method produced cell aggregates that only had a few bile duct-like structures and the tissue aggregates were mostly unviable. Neither of these two methods produced anatomically correct tissue structures, they were missing both bile duct-like structures and blood vessel-like structures. The cell aggregates that were grown in the Rotating Wall Vessel had 3D tissue aggregates with both bile duct-like structures and blood vessel-like structures, confirming that the Rotating Wall Vessel is the most effective method to grow hepatic tissue. Another study used this type of Rotating Wall Vessel to grow functional cardiac constructs to rehabilitate the functions of distressed rat heart (Nakazato, Taro, 2022). They seeded human-induced stem cell-derived cardiomyocytes (3D-hiPSC-CT) on fiber sheets and cultured them using a Rotating Wall Vessel and cultured a control group whose growing conditions were static. They transplanted the tissues into a myocardial infarction nude rat model and the performance of the two were evaluated. They determined that the 3D-hiPSC-CTs that were grown in the Rotating Wall Vessel had a 6% higher cell viability than that of the control group. The Rotating Wall Vessel group also had vastly improved contractile and electrical properties. When implanted in the nude rat model, the tissues from the Rotating Wall Vessel increased the overall cardiovascular performance of the heart. This

study provides insight on how this system can aid in the process of increasing the functional recovery of bio-organisms with a diseased heart. Another study used the Rotating Wall Vessel to engineer 3-D elastic cartilage in vitro to grow transplantable auricular cartilage (Takebe, T., et al., 2012). Samples were taken from microtia patients and were separated into cartilage and perichondrium layers. Cartilage progenitor cells (CPCs) were extracted from these samples and were seeded in pC-Hap/ChS scaffolding to prep them for culturing. The current methods of cranial reconstruction put a significant burden on the donors at the site of grafting and have an invariable absorption of the graft itself. The standard 2-D methods of grafting do not allow for much control of the size and shape due to the directional growth limitation caused by gravity. It was determined that culturing these CPCs in the Rotating Wall Vessel yielded much greater results than that of the standard 2-D method. The 3-D culture from the Rotating Wall Vessel had a much fuller shape and had proteoglycan and elastic fibers, which are exclusive extracellular matrices of elastic cartilage. This is evidence that this method of cellular cultivation is very effective in the reconstruction of complicated elastic cartilage structures. The Rotating Wall Vessel has been proven to accelerate and improve the process of differentiating pluripotent stem-cells into retinal organoids (DiStefano, Tyler J., et al, 2020). It has been shown that the stem cells grown in a Rotating Wall Vessel at day 25 are at a similar stage (if not further along) of organoid differentiation as stems cells grown in static conditions at day 32. This shows a significant improvement of the time it takes for the stem cells to mature into retinal organoids by using the Rotating Wall Vessel. The vast acceleration of this process could prove very useful in future study. Across many avenues of research, this Rotating Wall Vessel has become a very popular method of cell growth and maturation. This can be credited to its ability to create 3-D cultures due to its simulated microgravity environment.

2.3 Importance of Yeast in the RWV

Evolutionary mechanisms developed by all biology to combat the external pressure of gravity, such as mechanosensing, are altered in real and simulated microgravity conditions. Mechanosensing initially alters the cells extracellular matrix and cytoskeleton networks which signals for gene regulation for further adaptation (Po, Agnese, et al., 2019), (Grimm, Daniela, et al., 2014). The current models suggest that the decrease of gravitational pressure reduces the energy required by the cell to push back against gravity. This reduction of gravity allows for low energy shapes such as spheres which attributes to many of the advantages of growing cells in a Rotating Wall Vessel. While the phenotype is observed, the mechanism of cytoskeleton remodeling is not understood in microgravity. To determine how the cytoskeleton is adapting to microgravity conditions, the noise of the system must be reduced. Using a model system that does not form spheroids is necessary to reduce such noise. *Saccharomyces cerevisiae*, Baker's yeast undergoes minimal morphological changes and does not form 3D cultures inside the Rotating Wall Vessel, yet their cytoskeleton is altered similar to spheroid forming cells. Furthermore, yeast are commonly used to study the basic mechanisms of mammalian cells as they contain human homologs, many of which are studied in areas regarding human health (Kachroo, Aashiq H., et al., 2022), (Laurent, Jon M., et al., 2020). Therefore, their basic adaptive principles can be studied in simulated microgravity and applied to more complex multicellular systems.

2.4 Research Gap

There are multiple types of bioreactor vessels that are used to grow cell aggregates. The purpose behind using these systems is to reduce the shear stress experienced by the cells as they grow. This is done to replicate how cells would grow in microgravity under similar conditions where they would experience little shear stress. Most of these bioreactor vessels include some sort of inlet and outlet to keep a constant stream of fluid medium moving in and out of the vessel.

Due to this added flow, these types of vessels have been shown to have traces of Taylor-Couette vortices which is a type of turbulence. Any added turbulence to these systems will inevitably increase the amount of fluid shear that is experienced by the particles, thus allowing for a higher chance that some of the particles will be damaged. The NASA designed rotating wall vessel (Fig. 1) is a closed system that does not include any inflow or outflow, which in turn, eliminates the presence of these turbulent Taylor-Couette Vortices. This causes the vessel to have a laminar solid body rotation, which allows the particles to be suspended in the medium relative to the wall rotation, eliminating any unnecessary turbulent forces. As the vessel rotates, the buoyancy of the particles, as well as the centrifugal and Coriolis forces induced by the rotational motion allow the particles to achieve this suspended state. The suspension of the particles is key to the success of this device and is what allows them to experience “simulated microgravity”. Most of the research in this area focuses on the vessels with inflow and outflow, very few CFD simulations have been modeled after this type of rotating wall vessel with solid body rotation (SBR). The few that have focused on the shear stress on chitosan scaffolds (M.N. Cinbiz, R.S. Tıǧlı, I.G. Beşkardeş, M. Gümüşderelioǧlu, Ü., 2010) or the paths of particles around the vessel at different rotational speeds (Liu, T.Q., Li, X.Q., Sun, X.Y., Ma, X.H., Cui, Z.F., 2004). Neither of which talk about the acceleration that the particles experience while suspended in the vessel, which is the primary focus of this study.

CHAPTER III

METHODOLOGY

3.1 CFD Model

A CFD model of a rotating wall vessel with solid body rotation model was created using the program STAR-CCM+. A 0.1-inch plane with interfaces on both sides was modeled in the geometry builder (Fig. 2). The interface allows the cells to pass through one side and back in

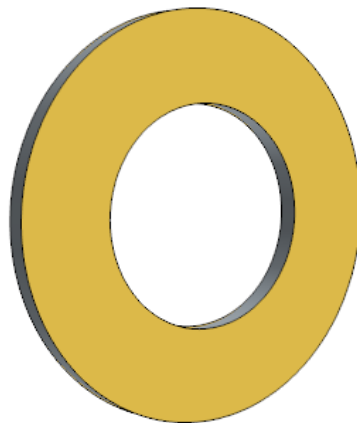


Figure 2: Geometry Scene of 0.1 in plane section

(like in PAC-MAN) resulting in a periodic boundary condition. This was done to avoid any unnecessary collisions with the plane section wall that would have otherwise been there if the interface was not implemented. The model uses laminar flow since the vessel being modeled is a closed system with solid body rotation, which eliminates all significant mechanisms that cause turbulence. A Lagrangian Multiphase model is used in order to calculate and track the particle

values within the fluid system. This model typically uses 4 phase interactions which are fluid-fluid, fluid-particle, particle-fluid, and particle-particle (A. Diggs, S. Balachandar, 2016). This means that all Lagrangian multiphase models must have at minimum these four phase interactions. The program already accounts for all the phases involving the fluid, so only two-phase interactions were set up. The first is simply the interactions between the particle (Particle-Particle). The second is the interactions between the outside walls and the particles (This is not part of the 4 key components, but it is still a necessary part for this set up). A parcel injector was used as the method of which the particle gets placed into the system. A table was made with the desired location that each particle would be placed in the system (using cylindrical coordinates). Four different variations of this simulation were made, and all ran in parallel. Each of the four has a row of eight particles that were situated at varying radial distances from the center (Figs 3-6). Simulations were made using the following radial distance from the center: 30 millimeters, 35 millimeters, 39 millimeters, and 43 millimeters; for the sake of this paper, we will assign them the names Sim 1, Sim 2, Sim 3, and Sim 4, respectively for ease of reference.

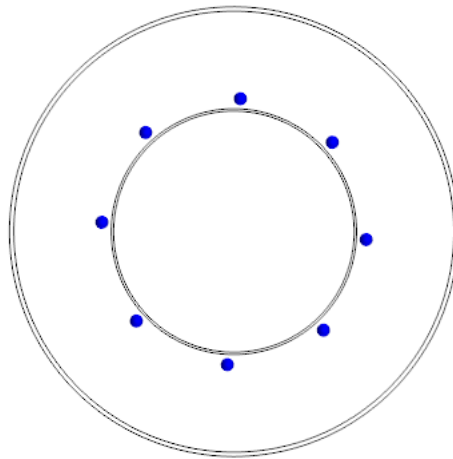


Figure 3: Sim 1 – Particle Orientation at radial distance $r = 30$ mm

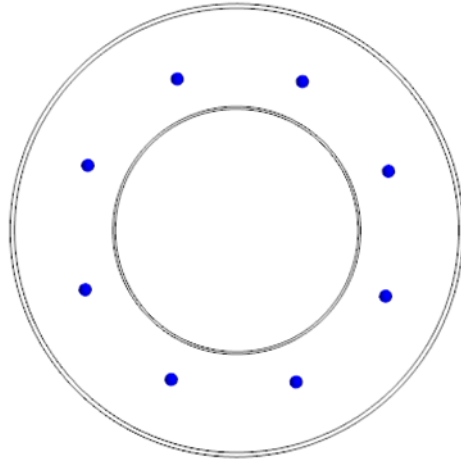


Figure 4: Sim 2 – Particle Orientation at radial distance $r = 35$ mm

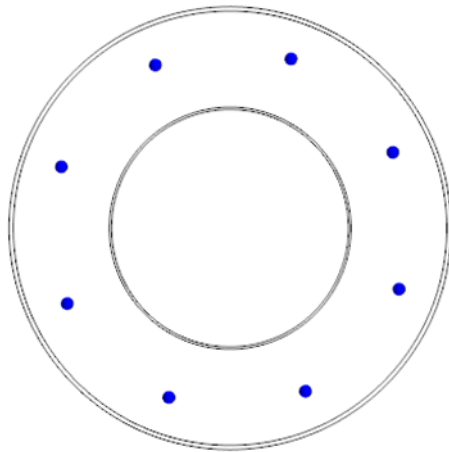


Figure 5: Sim 3 – Particle Orientation at radial distance $r = 39$ mm

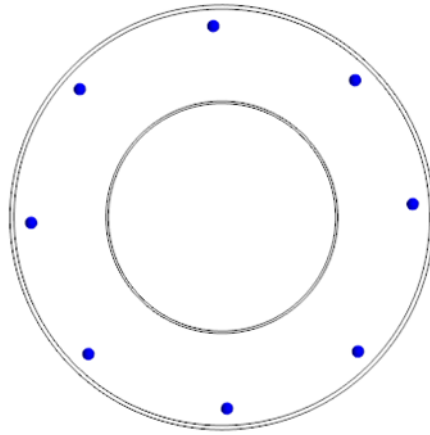


Figure 6: Sim 4 – Particle Orientation at radial distance $r = 45$ mm

This is so that the particles can be evaluated at any point in the vessel without having to run the simulation for a full rotation and so the data could be processed more effectively. The particles are placed after 0.001 seconds of run time. This is done because the model iterates every 0.001 seconds (0.001 second iteration time is used to achieve a higher level of accuracy), this allows the particles to be injected after the first-time step (the earliest time that the program allows particles to be injected). The particles were injected into a fully developed flow field that was determined in a previous simulation (Fig. 7). The initial conditions of the developed flow field were loaded using a table file. This was done to eliminate any unnecessary computational time that it would take to allow the fluid medium to reach a fully developed state. Each particle is assigned an Index number so every single one can be evaluated separately. The particles being used mimic the properties of Yeast Cells, which have a diameter of $1.2\mu\text{m}$, and density of 1112.6 kg/m^3 (Which is greater than that of water (999.7 kg/m^3)). Yeast cells

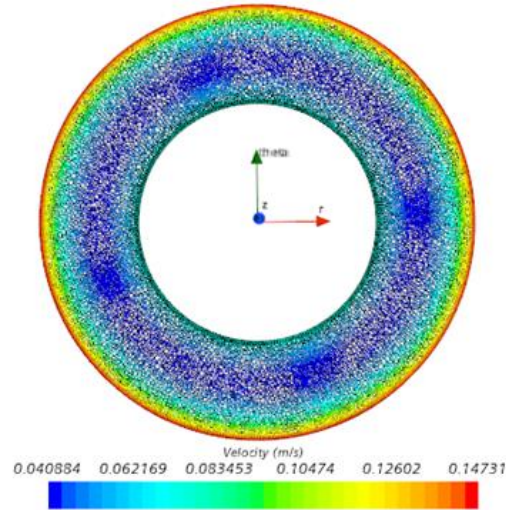


Figure 7: Fully Developed fluid domain without particles

do not have a perfectly cylindrical shape, but for the purpose of this simulation spherical particles were used. Spherical particles are the closest thing to the shape of actual yeast particles that the program allows to be used in particle injectors. A particle track file was used to keep a history of the particle values. This is a feature of the Lagrangian Multiphase model within STAR-CCM+ that tracks the particle values that are predetermined in the track file menu. Once the simulation is done iterating, it outputs a track file which can then be reuploaded into the program and used for data processing. A particle track is recorded when a particle crosses from one cell within the mesh to another (so the smaller the mesh, the more particle outputs would be recorded). The scalars that were tracked include time, particle count, and particle index. The vectors that were tracked include, parcel centroid, particle drag force, particle velocity. Particle acceleration was calculated from the particle track file data. The formula can be represented as:

$$a_{calc} = \frac{dV}{dt}$$

It can be expanded as

$$a_{calc} = \frac{V_f - V_i}{t_f - t_i}$$

where,

a_{calc} = *Calculated Acceleration*

V_f = *Final Velocity*

$V_{initial}$ = *Initial Velocity*

t_f = *Final Time*

t_i = *initial time.*

The mesh is very important to any CFD simulation, it is the means by which the fluid domain is calculated. The mesh must be the right size for the purpose of the simulation, and the user must select an economical mesh that provides the required degree of solution accuracy (Kang, C.-W., Wang, Y., et al, 2013). The meshers used include, Surface Remesher, Polyhedral Mesher, Prism Layer Mesher with a 1 mm base size and a 50% target surface size (relative to base) (Figs. 8-12). Also, each of the simulations have a refined area in accordance with the radial position of the particles. The refinement zones were meshed with a target absolute size of .06 meters. This was done to allow the particle to cross more mesh boundaries in order to get more data without increasing the computational demand too much.



Figure 8: Sim 1 – Mesh Scene for $r = 30$ mm



Figure 9: Sim 2 – Mesh Scene for $r = 35$ mm



Figure 10: Sim 3 – Mesh Scene for $r = 39$ mm



Figure 11: Sim 4 – Mesh Scene for $r = 43$ mm

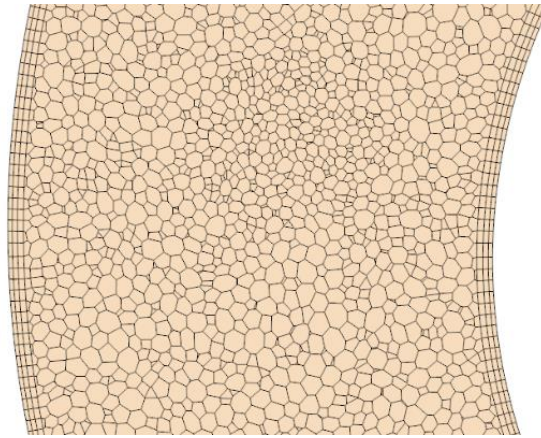


Figure 12: Mesh Scene – Prism Layers

The prism layers included 3 total prism layers with a total thickness of .7 mm (Fig. 12). With the given mesh settings, there are 1,440,860, 1,609,502, 1,772,625, 1,938,290 total cells in the mesh for Sim 1, Sim 2, Sim 3, & Sim 4, respectively. Since the particles are 12 μm in size, the mesh must be small enough to provide enough data points to ensure their values are accurate but also large enough to prevent a heavy computational time. The current settings were found to provide a nice balance of both accurate data points and reasonable computational time. The simulation is set to rotate at 30 rpm. 10- 60 rpms have been shown to provide the lowest amount of shear and make for optimal growing conditions (T. G. Hammond and J. M. Hammond). This means it will take 2 seconds of physical time to complete one full rotation. The time step was set to iterate every 0.001 seconds for solution accuracy. The time of 0.001 was found to be a good iteration time that will optimize that solution accuracy without making the computational demand too high. The extremely small particles that are being modeled give this simulation an extraordinarily high computational time. To combat this, the OSU HPCC PETE supercomputer was utilized because of its extremely fast computation rate. This would in turn reduce the amount of time it would take the simulation to run. This was a computer on 1 nodes,

which is the equivalent of 32 processing cores. The set up takes 5 days of computation time to achieve 1.6 seconds of solution time. This amount of time will be sufficient because the particles are placed evenly around the vessel, so that any particle can be analyzed at any given point during the rotation and simulating multiple rotations would just be redundant. Simulations are extremely powerful tools to help calculate phenomena within fluid systems, but when modeling something that has never been done before the only way to be 100% sure that it is set up correctly is to take some real-world measurements. Particle Image Velocimetry (PIV) is the only way to conduct a real-world experiment to achieve the results that this study is after. For these reasons, PIV will be used to conduct an experiment that will validate the set-up of the CFD Simulation.

CHAPTER IV

RESULTS & DISCUSSION

Particle track file data was read and processed to produce the following results. The following criteria will be presented and analyzed for each of the four simulations: Particle Deviation, Particle Acceleration vs Time, Particle Acceleration vs. Angular Position, and Standard Deviation of Acceleration Values across radial positions.

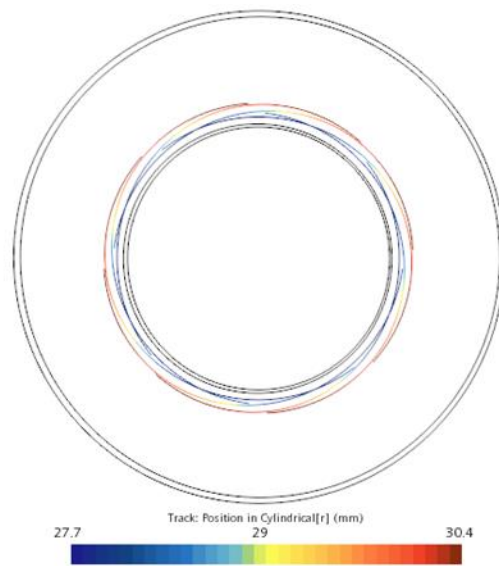


Figure 13: Sim 1 – Particle Radial Position Deviation $r = 30$ mm

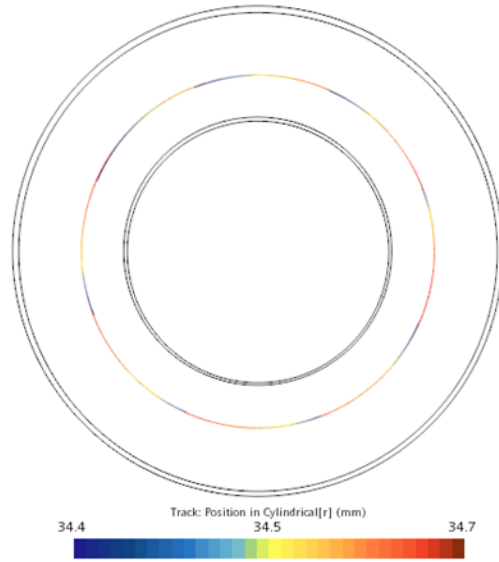


Figure 14: Sim 2 – Particle Position Deviation $r = 35$ mm

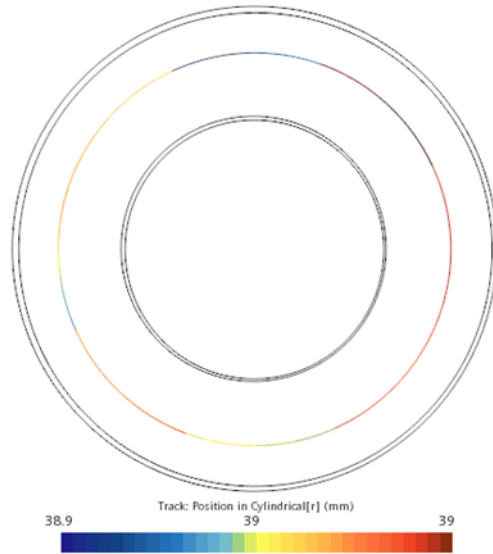


Figure 15: Sim 3 – Particle Position Deviation $r = 39$ mm

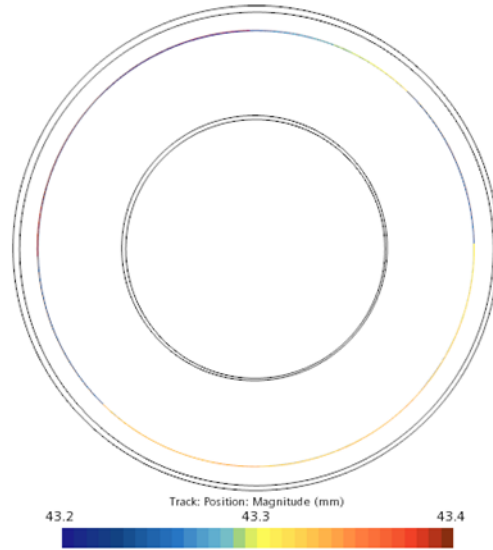


Figure 16: Sim 4 – Particle Position Deviation $r = 43$ mm

As shown in Figs. 14-16 the particles, when kept in constant rotation, do not have any significant deviations from their original radial positions. However, looking at Fig. 13, it can be observed that the particles deviate towards the inside of the vessel. This is likely from the higher fluid velocity close to the inner wall. Based on the figure, the particles moved from their original radial position of .03 meters to an ended radial position of .027 meters. This was over the course of 1.6 seconds, so it is probable that the particles will deviate further inwards as more time progressed.

Particle Acceleration was calculated by taking the derivative of the j component of the Particle Velocity with respect to time. The Particle Velocity [j] was taken from the particle track file data. Figures 17-20 show the Calculated Particle Acceleration vs. Time for each of the four simulations. Each of which is shown over the time interval 0 to 1.6 seconds and each color is representative of a different particle in that given radial position.

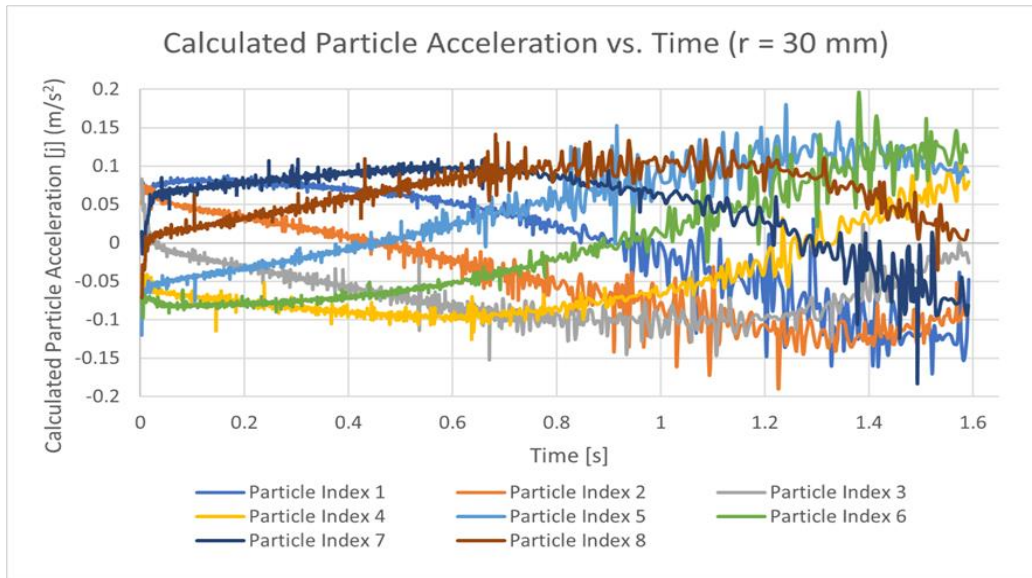


Figure 17: Sim 1 – Calculated Particle Acceleration vs. Time $r = 30$ mm

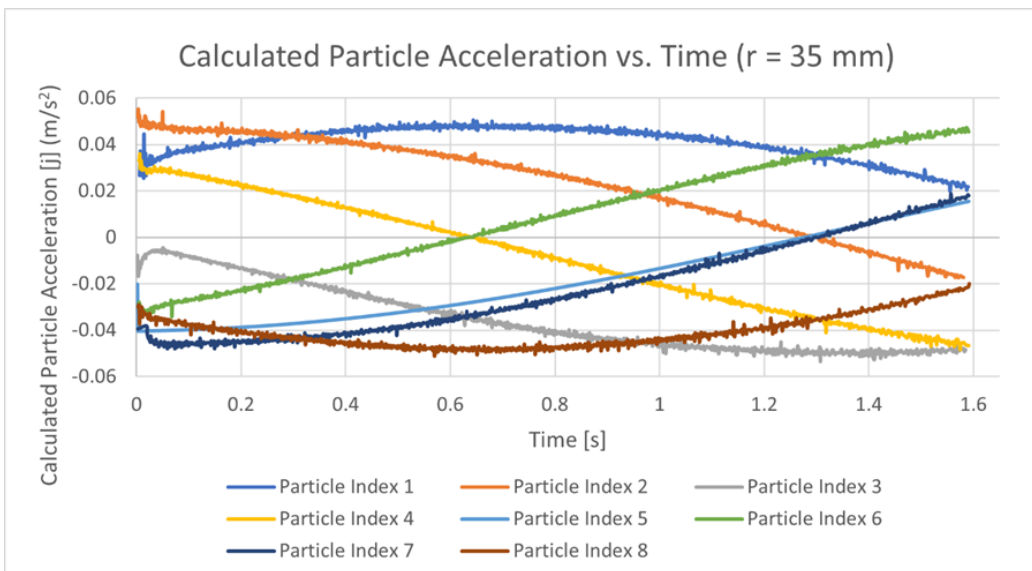


Figure 18: Sim 2 – Calculated Particle Acceleration vs. Time $r = 35$ mm

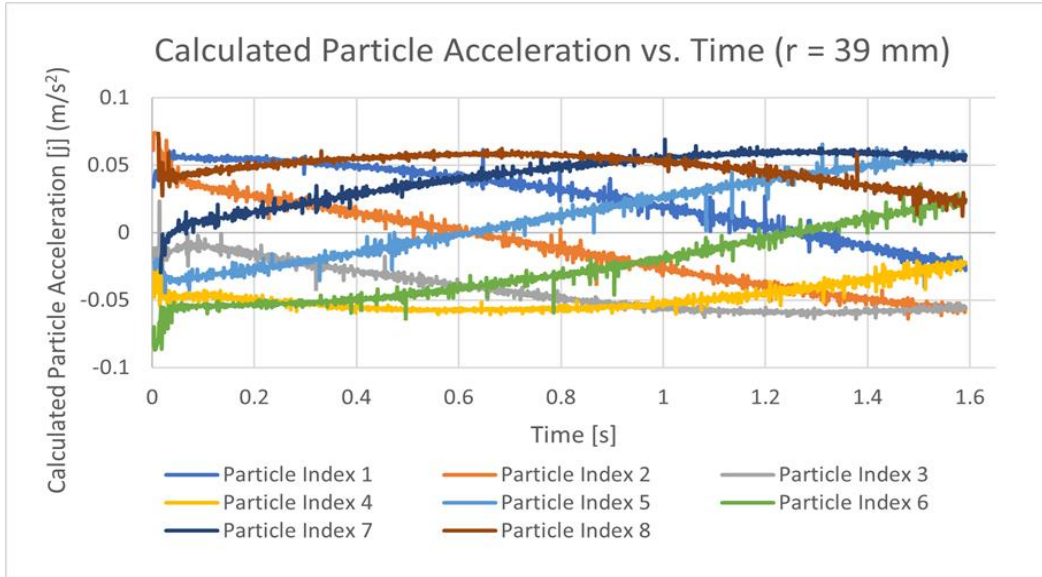


Figure 19: Sim 3 – Calculated Particle Acceleration vs. Time $r = 39$ mm

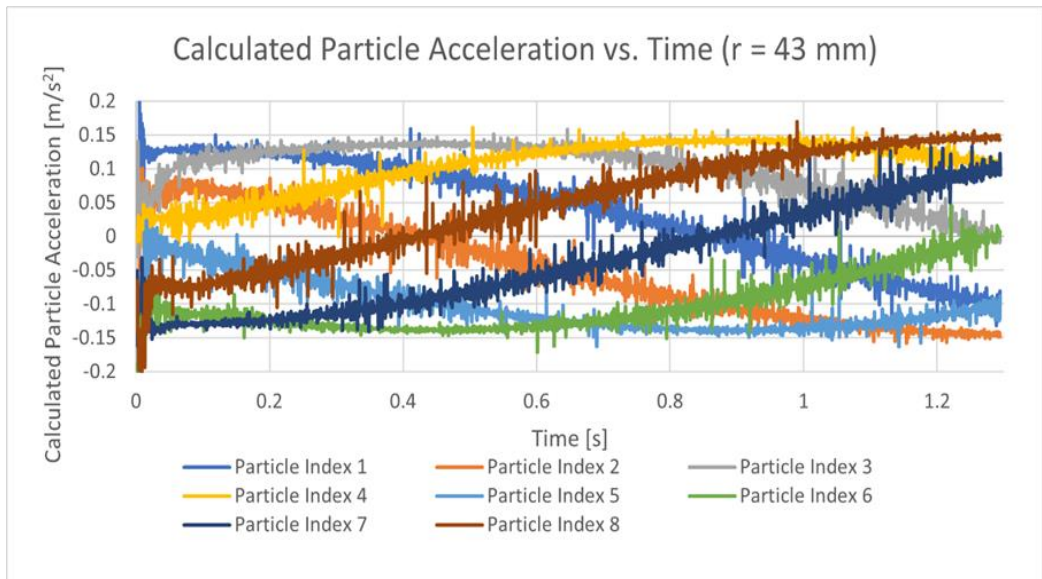


Figure 20: Sim 4 – Calculated Particle Acceleration vs. Time $r = 43$ mm

As you can see from Fig 17, the particle acceleration [j] predominately fluctuates between .1 and -1 m/s² for radial position .03 meters. Once the time reaches around the .7 second mark, the acceleration values slowly become more erratic and deviate more, reaching acceleration values that fluctuate between .2 and -2 m/s². Referring back to Fig. 13, we can conclude that the spike in particle acceleration in this radial position is due to the particle's deviation towards the inner wall. This is an indication that the particles experience more turbulence as they approach the inner wall of the vessel. The data on Figure 18 for the radial position of .035 meters is extremely consistent and stays perfectly between an acceleration range of .05 to -.05 m/s². These particles are situated more towards the middle and have very little deviation in acceleration. This is likely due to the lower fluid velocity in the region (Fig. 7), which in turn leads to less turbulence induced on the particles. For the radial position of .039 meters, the acceleration values mainly stay between the range of .06 and -.06 m/s². The fluid velocity is slightly higher in this region than that of the region that correlates to the particles at the radial position of .035 m. This is the reason for the slight increase of min and max acceleration and why there is slightly more deviation in the values. Looking at Figure 20, for the .043-meter radial position, we can see that the particle acceleration ranges from .12 to -.12 m/s². The data for this position is much more erratic and the values deviate much more than the previous cases. Again, this is directly correlative of the local fluid velocity. Looking at Figure 7 again, the fluid velocity in this area is the highest, making this region have the highest particle acceleration and the highest amount of turbulence. This data gives a very thorough understanding of how the radial position of the particles within the rotating vessel affects their acceleration. On top of this, it is also important to understand how the angular position of the particles affects their acceleration.

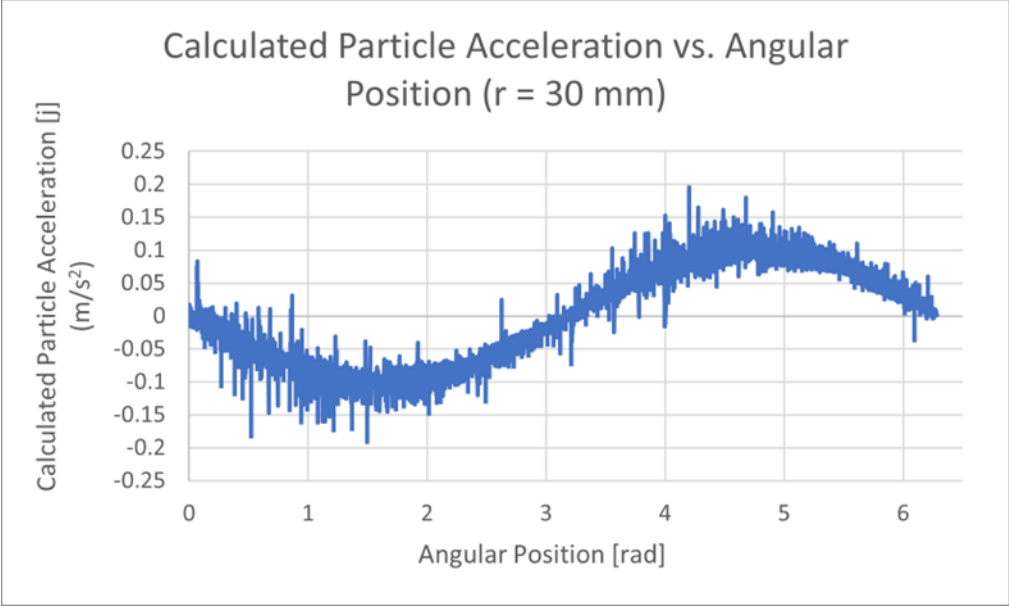


Figure 21: Sim 1 – Calculated Particle Acceleration vs. Angular Position r = 30 mm

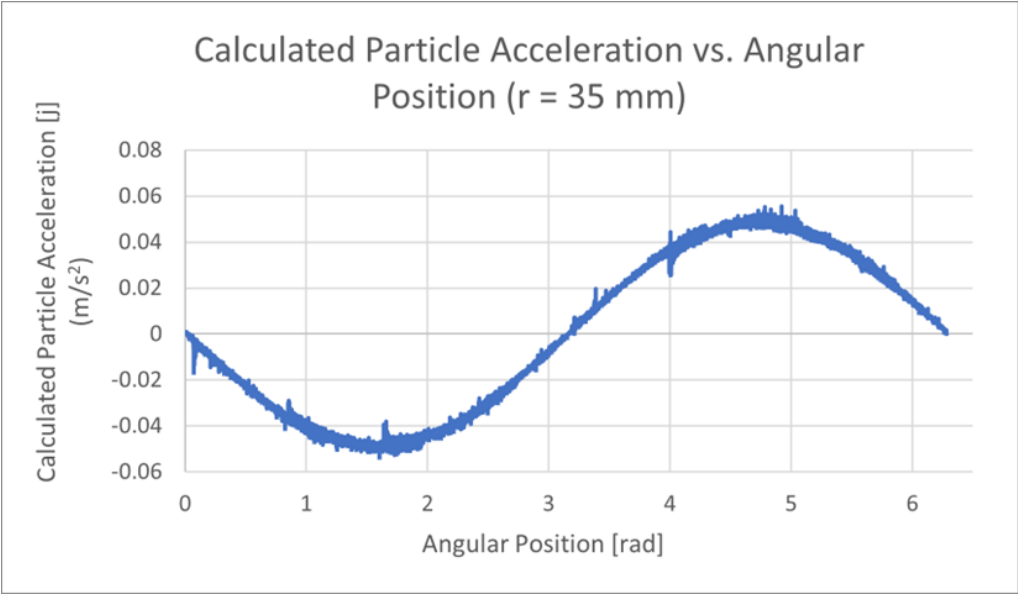


Figure 22: Sim 2 – Calculated Particle Acceleration vs. Angular Position r = 35 mm

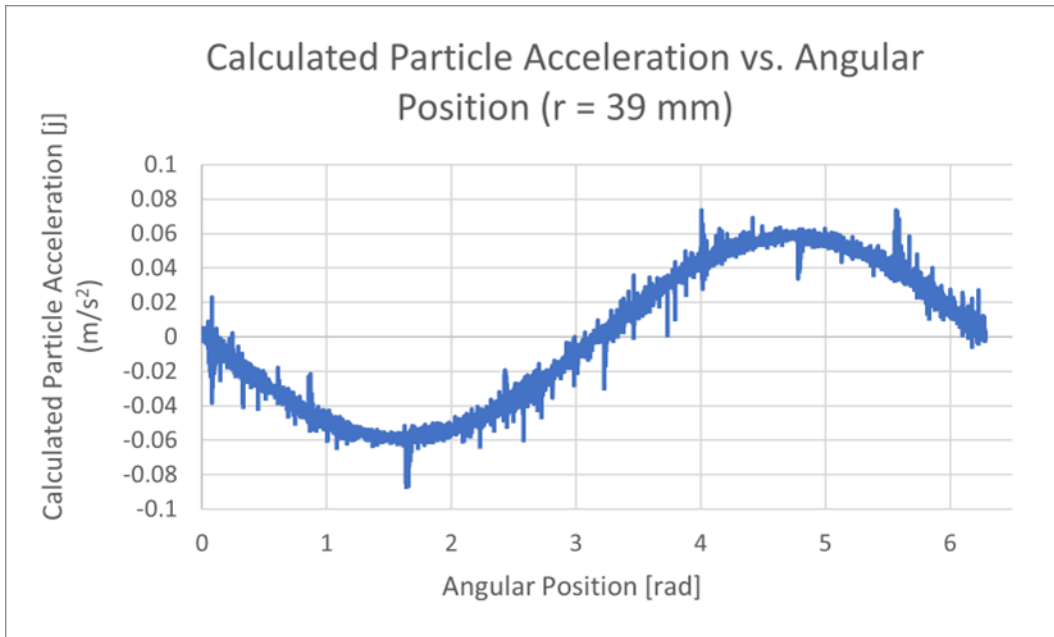


Figure 23: Sim 3 – Calculated Particle Acceleration vs. Angular Position $r = 39$ mm

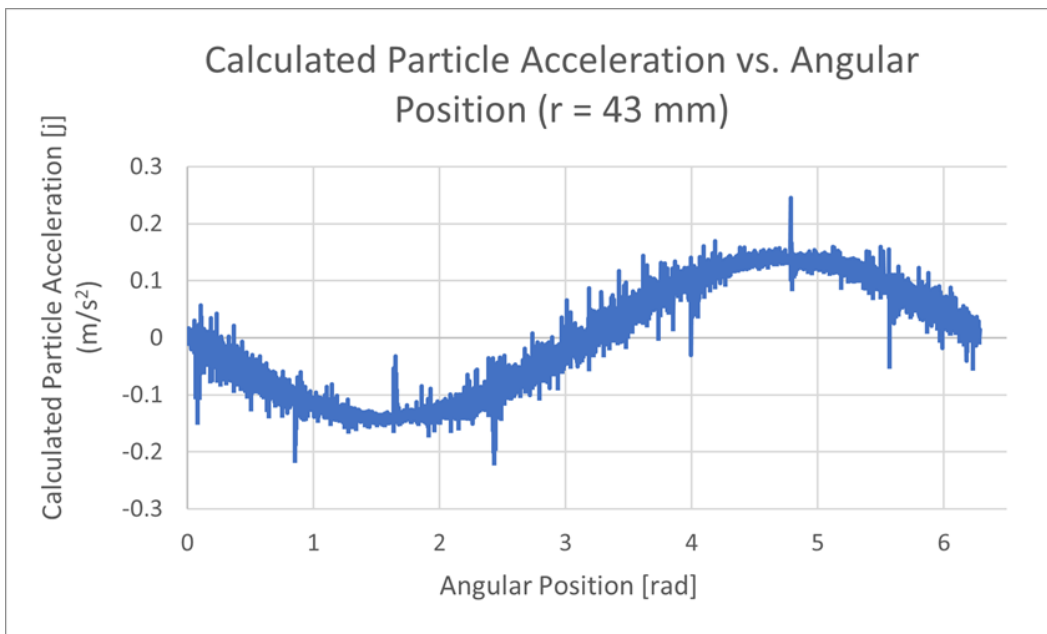


Figure 24: Sim 4 – Calculated Particle Acceleration vs. Angular Position $r = 43$ mm

Figures 21- 24 show the acceleration of the particles for each of the four cases as they pass through the different angular positions of the vessel. Angular position is represented in radians

and shows the range from 0 to 6.2 (0 to 360 degrees). This allows for the acceleration of the particles to be observed at any point during the rotation of the device. The results in Figures 21 - 24 align very closely with the data represented by Figures 17 – 20. The minimum and maximum acceleration for each radial position remains largely the same in both data sets. However, the Acceleration vs. Time graphs, while able to show data for each individual particle, are not able to distinguish exactly where the particles are within the given radial position. Figures 21 – 24 can give more insight of how the angular position affects the particles acceleration values. In any case, the acceleration is the lowest at 0, 3.14, and 6.28 rads, where 0 and 6.28 rads are the same position. These are the only points where the particles are able to experience an acceleration of true zero, while every other angular position in the vessel can only get extremely close.

A static version of the .035 radial position simulation was run to test the continuity and validity of the other simulations. The goal was to compare the vertical particle displacement from the simulation data against the calculated particle displacement over a certain time period. Static conditions were used so that an acceleration of 0 m/s² in the y direction can be assumed for the calculated values. The displacement of the particle can be calculated from the formula written as

$$s = vt$$

Where,

s = Particle Displacement

t = Time

and the formula for particle velocity is written as

$$V = \frac{D^2(\rho_y a + \rho_y g - \rho_f g)}{18 \mu}$$

Where $a = a = 0 \text{ m/s}^2$,

$$V = \frac{D^2(g(\rho_y - \rho_f))}{18 \mu}$$

where,

D = Particle Diameter

g = Gravitational Constant of Earth

ρ_y = Density of Yeast Particles

ρ_f = Density of Culture Fluid

μ = Culture Fluid Viscosity

Table 1: Static Sim -Particle Displacement vs Calculated Particle Displacement [μm]

Static Simulation Particle Displacement vs Calculated Particle Displacement [μm] @ t = 2s								
Particle Index	1	2	3	4	5	6	7	8
Calculated Particle Displacement [μm]	18.3	18.3	18.3	18.3	18.3	18.3	18.3	18.3
Static Sim Particle Displacement [μm]	18.7	15.5	17.8	18.1	18.5	17.8	18.2	17.5
Percent Difference [%]	2%	15%	3%	1%	1%	3%	1%	4%

Table 1 shows the Vertical Particle Displacement that was derived using the particle track files that were output from the static situation. The displacement values from each of the eight particle indices are shown. These values are pulled after the simulated had run for 2 seconds of physical time. The calculated particle Displacement was determined by using the displacement and velocity formulas as listed above. 2 seconds was used as the time value to mimic the physical time used by the displacement values given by the simulation. On average, the Particle Displacement values fall within 3.87% of the calculated values.

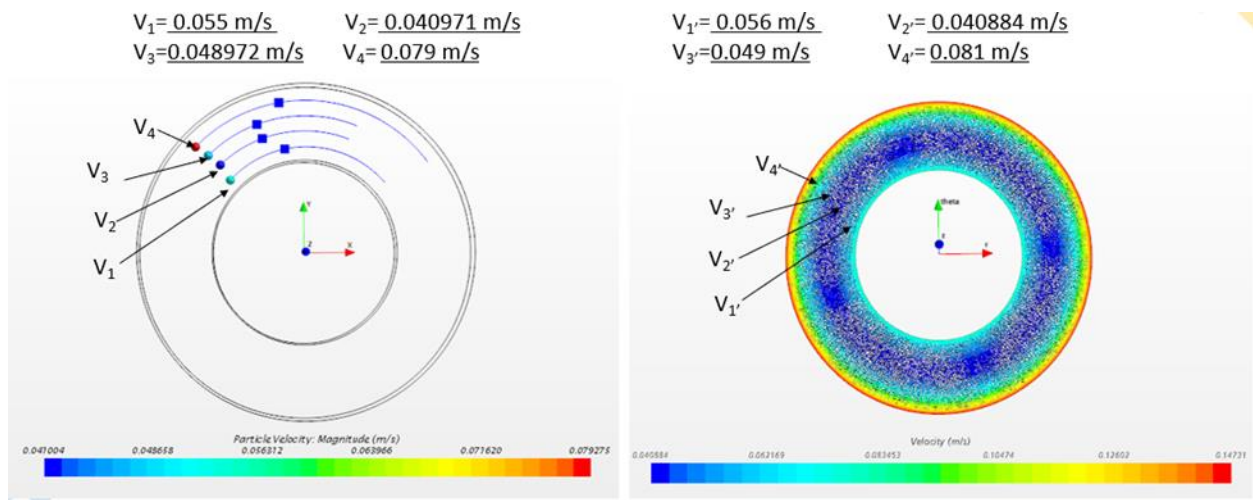


Figure 25: Comparing Particle Velocity to Fluid Regime Velocity (Magnitude)

Looking at figure 25, it can be observed that the velocity magnitude of the particles stays relatively constant for every radial distance (rd) away from the center. This is largely due to the reasoning that the particles are moving at the same rate as the local fluid velocity. Figure 8 shows the velocity of a particle (V_n) from each radial distance compared to that of the velocity of the fluid medium (V_n') at the same region. Once again referencing figure 8, $V_1 = 0.055 \text{ m/s}$ while $V_{1'} = 0.056$. The other corresponding V and V' values are extremely close in value as well, this lines up with the results that were found in (Wereley ST, Akonur A, Lueptow, 2002) and as stated in (M.N. Cinbiz, R.S. Tıǧlı, et al, 2010), meaning that it is an incompressible flow. The

velocity is the highest near the inner and outer walls as can be seen in both Fig. 7 & 8. The reason behind this is that the walls are the driving mechanism that transfers the velocity to the fluid and the particles, so the near wall velocity of the fluid moves at almost the same speed at the walls, while the velocity of the fluid decreases as the distance from the wall increases. Once this simulation is run for the full two seconds, it is hypothesized that both the particle and the fluid velocities will remain extremely close to one another. This is because it has been shown to have incompressible flow.

The results across all the data sets point to the same conclusion that the particle experience the most turbulence resulting in the highest acceleration values when they are closest to the outer and inner walls. Figure 26 shows the standard deviation of the Calculated acceleration values across all four radial positions. This is a good representation of the turbulence experienced by the particles in the various positions in relation to one another. It supports the conclusion that the walls generate the most turbulence and that the areas in the center of these two walls offer the

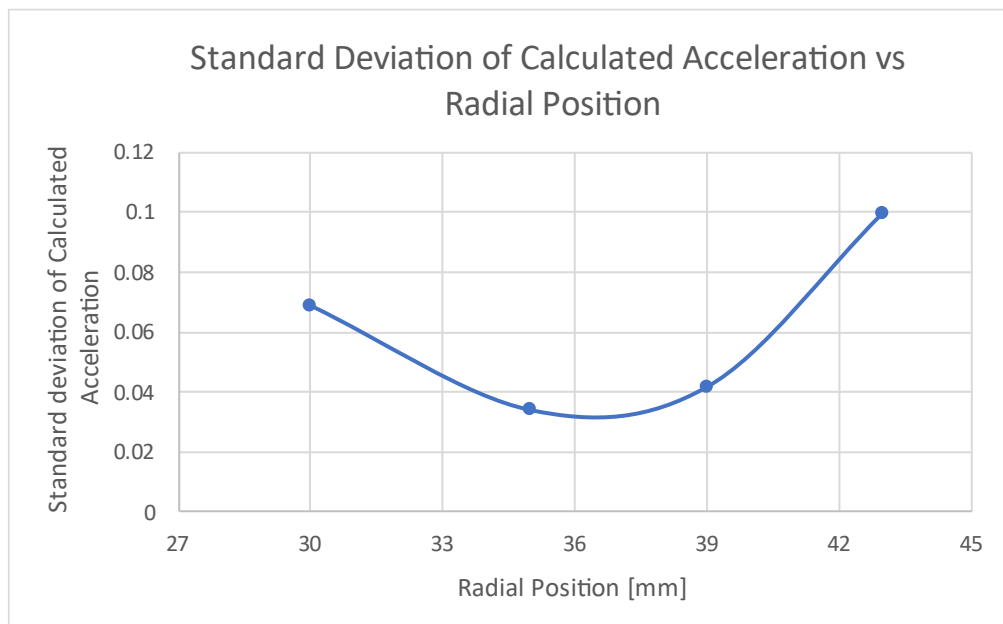


Figure 26: Standard Deviation of Calculated Acceleration vs Radial Position

most ideal growing conditions. From this data, finding the relationship between particle path position, fluid velocity, and particle acceleration was able to successfully provide not only absolute minimum and maximum particle acceleration [j] values for the unit as a whole, but also was able to determine what areas of the vessel offer the most ideal conditions. This, however, was only done for the single rotation speed; further studies can be done to mimic this process for any given rotational speed.

CHAPTER V

CONCLUSION

In this study, we have presented and discussed the finding of four CFD simulations, whose purpose was to measure the acceleration values of yeast particles in a Rotating wall vessel to see what percentage of Earth's gravity is imparted on the particles. From the results, it can be concluded that the vessel can eliminate from 98.5% to 100% of the acceleration experienced due to gravity, depending on what part of the vessel the particles are in. They experience the lowest acceleration towards the center of the vessel and the most towards the inner and outer wall, where there is more fluid shear. This work provides a deeper insight into the physics at work inside Rotating Wall Vessels that can be applied to future work with RWVs.

5.1 Future Work

5.11 PIV (Particle Image Velocimetry)

Particle image velocimetry is a frequent practice that is often used to validate CFD results. This method consists of reflective beads that flow in the given system that is being modeled, then a laser is shone at them and reflected for the high-speed camera to capture as images. The images can then be processed, where the multiple frames can be analyzed. The displacement of the particles over a certain time period determines the particles' velocity, then the change in velocity of the particle over another period of time can be used to determine acceleration. These values can then be compared to that of the results of this study. The actual vessel cannot be used for this process because the front portion is solid, therefore a laser cannot

be shone through. A custom vessel will need to be constructed that has a translucent endcap. This vessel would mimic the actual RWV in every aspect except that it should have a customized endcap. Future research can be conducted using two approaches, one where the laser points towards the front of the vessel (the translucent endcap), the other with the laser pointed at the side. Quantities such as velocity and acceleration can be calculated based off the displacement of the beads as observed by the images captured by the high-speed camera. These calculated values could serve as a validation experiment for data that is obtained and shared using the CFD simulations of this research.

5.12 Framework To Test Different Experimental Set-Ups

This research can also serve as a groundwork template for further research where simple changes can be made to test different types of cells with differing densities and sizes. The simulation can be changed to run at different speeds to find a correlation between the rotation speed and the percentage of gravity experienced by the particles. Also, different parameters such as particle concentration and particle density could also be implemented to see if that has any effect on the amount of acceleration they experience.

REFERENCES

- A. Diggs, S. Balachandar Evaluation of methods for calculating volume fraction in Eulerian–Lagrangian multiphase flow simulations *J. Comput. Phys.*, 313 (2016), pp. 775-798.
- D.W. Hutmacher, H. Singh, Computational fluid dynamics for improved bioreactor design and 3d culture *Trends Biotechnol.*, 26 (4) (2008), pp. 166-172
- DiStefano, Tyler J., et al. “Accelerated and Improved Differentiation of Retinal Organoids from Pluripotent Stem Cells in Rotating-Wall Vessel Bioreactors.” *Stem Cell Reports*, vol. 16, no. 1, 2021, p. 224., <https://doi.org/10.1016/j.stemcr.2020.12.006>.
- Figueredo-Cardero, A., Chico, E., Castilho, L. and de Andrade Medronho, R. (2012), Particle image velocimetry (PIV) study of rotating cylindrical filters for animal cell perfusion processes. *Biotechnol Progress*, 28: 1491-1498. <https://doi-org.argo.library.okstate.edu/10.1002/btpr.1618>
- Figueredo-Cardero, A., Martínez, E., Chico, E., Castilho, L.R. and Medronho, R.A. (2014), Rotating cylindrical filters used in perfusion cultures: CFD simulations and experiments. *Biotechnol Progress*, 30: 1093-1102. <https://doi.org/10.1002/btpr.1945>
- Fukuda, Ana Paula, et al. “Simulated Microgravity Accelerates Aging in *Saccharomyces Cerevisiae*.” *Life Sciences in Space Research*, vol. 28, 2021, pp. 32–40., <https://doi.org/10.1016/j.lssr.2020.12.003>.
- Grimm, Daniela, et al. “Growing Tissues in Real and Simulated Microgravity: New Methods for Tissue Engineering.” *Tissue Engineering Part B: Reviews*, vol. 20, no. 6, 2014, pp. 555–566., <https://doi.org/10.1089/ten.teb.2013.0704>.
- Ishikawa, Momotaro, et al. “Reconstitution of Hepatic Tissue Architectures from Fetal Liver Cells Obtained from a Three-Dimensional Culture with a Rotating Wall Vessel Bioreactor.” *Journal of Bioscience and Bioengineering*, vol. 111, no. 6, 2011, pp. 711–718., <https://doi.org/10.1016/j.jbiosc.2011.01.019>.
- Kachroo, Aashiq H., et al. “Humanized Yeast to Model Human Biology, Disease and Evolution.” *Disease Models & Mechanisms*, vol. 15, no. 6, 2022, <https://doi.org/10.1242/dmm.049309>.
- Kang, C.-W., Wang, Y., Tania, M., Zhou, H., Gao, Y., Ba, T., Tan, G.-D.S., Kim, S. and Leo, H.L. (2013), Computational fluid modeling and performance analysis of a bidirectional rotating perfusion culture system. *Biotechnol Progress*, 29: 1002-1012. <https://doi.org/10.1002/btpr.1736>

- Laurent, Jon M., et al. "Humanization of Yeast Genes with Multiple Human Orthologs Reveals Functional Divergence between Paralogs." *PLOS Biology*, vol. 18, no. 5, 2020, <https://doi.org/10.1371/journal.pbio.3000627>.
- Liu, T.Q., Li, X.Q., Sun, X.Y., Ma, X.H., Cui, Z.F., 2004. Analysis on forces and movement of cultivated particles in a rotating wall vessel bioreactor. *Biochem. Eng. J.* 18, 97–104.
- M.N. Cinbiz, R.S. Tıgılı, I.G. Beşkardeş, M. Gümüşderelioğlu, Ü. Çolak Computational fluid dynamics modeling of momentum transport in rotating wall perfused bioreactor for cartilage tissue engineering *J. Biotechnol.*, 150 (2010), pp. 389-395
- Menter, F. R. "Two-Equation Eddy-Viscosity Turbulence Models for Engineering Applications." *AIAA journal* 32.8 (1994): 1598–1605. Web.
- Nakazato, Taro, et al. "Engineered Three-Dimensional Cardiac Tissues Maturing in a Rotating Wall Vessel Bioreactor Remodel Diseased Hearts in Rats with Myocardial Infarction." *Stem Cell Reports*, vol. 17, no. 5, 2022, pp. 1170–1182., <https://doi.org/10.1016/j.stemcr.2022.03.012>.
- Po, Agnese, et al. "Phenotypic Transitions Enacted by Simulated Microgravity Do Not Alter Coherence in Gene Transcription Profile." *Npj Microgravity*, vol. 5, no. 1, 2019, <https://doi.org/10.1038/s41526-019-0088-x>.
- Razieh Jalalabadi, Jongmin Kim & Hyung Jin Sung (2017) Turbulent structures in an optimal Taylor–Couette flow between concentric counter-rotating cylinders, *Journal of Turbulence*, 18:5, 480-496, DOI: 10.1080/14685248.2017.1296959
- Schwarz RP, Goodwin TJ, Wolf DA. Cell culture for three-dimensional modeling in rotating-wall vessels: an application of simulated microgravity. *J Tissue Cult Methods*. 1992;14(2):51-7. doi: 10.1007/BF01404744. PMID: 11541102
- Takebe, T., et al. "Human Elastic Cartilage Engineering from Cartilage Progenitor Cells Using Rotating Wall Vessel Bioreactor." *Transplantation Proceedings*, vol. 44, no. 4, 2012, pp. 1158–1161., <https://doi.org/10.1016/j.transproceed.2012.03.038>.
- T. G. Hammond and J. M. Hammond
Optimized suspension culture: the rotating-wall vessel *American Journal of Physiology-Renal Physiology* 2001 281:1, F12-F25
- Wei, L., Diao, Y., Qi, J., Khokhlov, A., Feng, H., Xing, Y., & Li, Y. (2013). Effect of change in spindle structure on proliferation inhibition of osteosarcoma cells and osteoblast under simulated microgravity during incubation in rotating bioreactor. *PLoS One*, 8(10) doi:<http://dx.doi.org/argo.library.okstate.edu/10.1371/journal.pone.0076710>
- Wereley ST, Akonur A, Lueptow RM. Particle fluid velocities and fouling in rotating filtration of a suspension. *J Membr Sci*. 2002;209:469–484.

Wolf DA and Schwartz RP. Analysis of Gravity-Induced Particle Motion and Fluid Perfusion Flow in the NASA-Designed Rotating Zero-Head-Space Tissue Culture Vessel. Washington, DC: 1991. (NASA Tech. Paper 3143)

Zakharov, Maksim, and Matthias Reuss. "Cell Size and Morphological Properties of Yeast *Saccharomyces Cerevisiae* in Relation to Growth Temperature." *FEMS Yeast Research*, vol. 18, no. 6, 2018, <https://doi.org/10.1093/femsyr/foy052>.

VITA

Devin Michael Jurko

Candidate for the Degree of

Master of Science

Thesis: DETERMINATION OF THE QUANTITY OF EARTH'S GRAVITY
IMPARTED ON PARTICLES IN A ROTATING CYLINDER FLUID
REGIME BASED ON PARTICLE DENSITY AND ROTATION SPEED

Major Field: Master of Science in Engineering Technology in Mechatronics and Robotics

Education:

Completed the requirements for the Master of Science in Mechatronics and Robotics at Oklahoma State University, Stillwater, Oklahoma in May, 2023.

Completed the requirements for the Bachelor of Science in Mechanical Engineering Technology at Oklahoma State University, Stillwater, Oklahoma in 2023.